Ceramics International xxx (xxxx) xxx–xxx

Contents lists available at ScienceDirect

Ceramics International

journal homepage: www.elsevier.com/locate/ceramint

Thermal properties of RE_2AlTaO_7 (RE = Gd and Yb) oxides

Chen Xiaoge[a], Zhang Hongsong[b], Liu Yanxu[b], Zhao Yongde[c], Ren Bo[b], Tang An[b], Lu Kui[d,*]

[a] Department of Civil Engineering, Henan University of Engineering, Zhengzhou 451191, PR China
[b] Department of Mechanical Engineering, Henan University of Engineering, Zhengzhou 451191, PR China
[c] Institute of Chemistry Henan Academy of Science, Zhengzhou 450001, PR China
[d] School of Chemical Engineering and Food Science, Zhengzhou Institute of Technology, Zhengzhou 450044, PR China

ARTICLE INFO

Keywords:
Thermal barrier coatings
Rare earth-aluminum-tantalum oxides
Thermal conductivity
Thermal expansion coefficient

ABSTRACT

In the current paper, the synthesis of RE_2AlTaO_7 (RE = Gd and Yb) oxides was performed through a high-temperature sintering method using Gd_2O_3, Yb_2O_3, Al_2O_3 and Ta_2O_5 as raw chemicals. The phase-structure, micro-morphology and thermal-physical properties of RE_2AlTaO_7 (RE = Gd and Yb) oxides were analyzed. The RE_2AlTaO_7 (RE = Gd and Yb) oxides exhibit single pyrochlore-type crystal-structure. Compared to Yb_2AlTaO_7, the Gd_2AlTaO_7 has greater thermal conductivity owning to relatively weaker phonon scattering. Because of higher electro-negativity of Yb, the Yb_2AlTaO_7 has lower coefficient of thermal expansion than Gd_2AlTaO_7. The RE_2AlTaO_7 (RE = Gd and Yb) oxides also exhibit no phase-transition between ambient and 1473 K.

1. Introduction

The yttria-stabilized zirconia (YSZ)- based thermal barrier coatings (TBCs), have been used to provide thermal-insulation protection for key-metal parts of gas turbines [1–3]. However, YSZ can not undertake long-term applications due to its inherent phase-transformation above 1473 K. Thus, exploration about novel candidates for TBCs is of great importance [4–6]. For thermal barrier coatings, the candidates should possess low thermal conductivity, appropriate coefficient of thermal expansion (CTE) and remarkable high-temperature phase-stability [7–9].

Recently, a few of compounds containing tombarthite-aluminum elements have received great attentions because of their eminent thermal physical properties. For example, the average CTE for Y_2O_3-Al_2O_3-SiO_2 is about 5×10^{-6}/K, its thermal conductivity (1.3 W/m K) is almost constant over the entire temperature range [10]. The $Y_4Al_2O_9$ shows low Young's modulus and thermal conductivity [11], and its thermal-conduction ability can be weakened by metal-cation doping [12]. The excellent bonding-strength and thermal-insulation capability for $Y_3Al_5O_{12}$-Al_2O_3 coatings can be put down to its good inoxidizability [13]. Ren et al. evaluated that the $LaCuAl_{11}O_{19}$, $La_2Zr_2O_7$-$LaCuAl_{11}O_{19}$ and $La_2Zr_2O_7$-$LaAlO_3$ have remarkable thermal-insulation ability from 473 K to 1473 K [14]. Compared to YSZ, the $Ln_2SrAl_2O_7$ oxides have greater volume thermal expansion coefficients and better heat-insulation ability [15]. The $LnMgAl_{11}O_{19}$ ceramics prepared by spark plasma sintering exhibit relatively high CTEs, and their thermal conductivities at 1473 K decrease with elevating tombarthite-cation radius [16]. Wan et al. indicated that the Ba_2DyAlO_5 has more-excellent thermo-physical performance [17]. The average thermal conductivity and CTE of La_2AlTaO_7 are 1.71 W (m K)$^{-1}$ and 8.2×10^{-6} K^{-1} [18].

However, the thermal properties of RE_2AlTaO_7 (RE = Gd and Yb) oxides have not been reported openly up to now. In this paper, the RE_2AlTaO_7 (RE = Gd and Yb) oxides were obtained through solid state reaction method, the crystal-type and thermo-physical properties were studied.

2. Experimental

In this manuscript, Gd_2O_3(purity ≥ 99.9%), Yb_2O_3(purity ≥ 99.9%), Al_2O_3(analytically pure) and Ta_2O_5(purity ≥ 99.9%) were selected as original chemicals. The weighted powders were fully mixed for 6 h using a milling pot with ethanol. After sufficient drying and sieving, the powder mixtures were uniaxially formed into disc samples at 10 MPa, and then the disc samples were further densified via cold-isostatic pressing under 200 MPa. The pressed samples of RE_2AlTaO_7 (RE = Gd and Yb) oxides were firstly sintered two times at 1673 K for ten hours accompanied by middle regrinding, and the ultimate products were pressureless sintered at 1873 K for ten hours.

The crystal-structure of RE_2AlTaO_7 (RE = Gd and Yb) oxides was identified via the X-ray diffractometry (XRD) (Bruker, D8 Advance). The actual density (ρ) test of final bulk samples was performed via Archimedes method. The surface micro-morphology observation of RE_2AlTaO_7 (RE = Gd and Yb) oxides was executed by scanning electron microscopy (SEM, FEI Quanta-250). According to the reference

* Corresponding author.
E-mail address: zhsandchen@126.com (L. Kui).

https://doi.org/10.1016/j.ceramint.2018.03.113
Received 27 January 2018; Received in revised form 13 March 2018; Accepted 13 March 2018

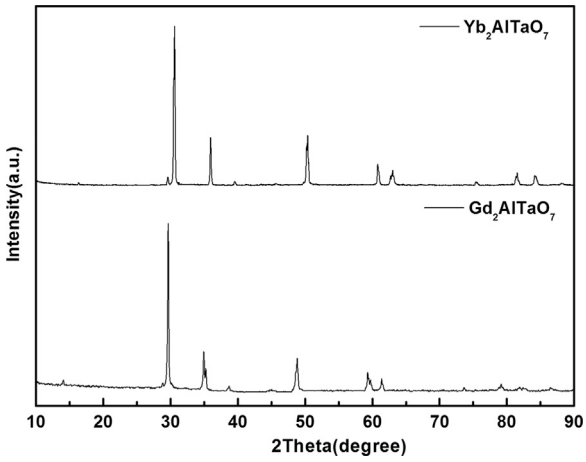

Fig. 1. XRD spectra for RE_2AlTaO_7 (RE = Gd and Yb) oxides.

specific heat capacities of Gd_2O_3, Yb_2O_3, Al_2O_3 and Ta_2O_5, the specific heat capacity (C_p) of RE_2AlTaO_7 (RE = Gd and Yb) oxides was computed via Neumann-Kopp rule. The CTE measurement for RE_2AlTaO_7 (RE = Gd and Yb) samples about 4 mm × 4 mm × 14 mm was carried out via a high-temperature dilatometer (Netzsch DIL 402C). The thermal diffusivity (λ) of the samples about Φ12.7 mm × 1 mm was determined by laser-flash technology on the automated LFA-427 instrument(Netzsch) in high-purity argon atmosphere. The thermal diffusivity measuring experiments were carried out in the temperature range of 493–1273 K. The thermal conductivity (k) of the bulk ceramics was calculated by Eq. (1) [16], which was further corrected by Eq. (2) [16]. Where k_0 and φ represent the actual thermal conductivity and porosity of RE_2AlTaO_7 (RE = Gd and Yb) oxides.

$$k = C_p \cdot \rho \cdot \lambda \tag{1}$$

$$\frac{k}{k_0} = 1 - (\frac{4}{3})\phi \tag{2}$$

3. Results and discussion

Fig. 1 presents the XRD patterns of RE_2AlTaO_7 (RE = Gd and Yb) oxides. It can be observed that the number and location of X-ray diffraction peaks for obtained bulks resemble that of $Sm_2Zr_2O_7$, which confirms a single phase composition with pyrochlore structure [19]. Compared to Gd_2AlTaO_7, the XRD peaks of Yb_2AlTaO_7 shift to higher angle because of minor radius of ytterbium-cation. The synthesized RE_2AlTaO_7 (RE = Gd and Yb) oxides can be regarded as the $A_2B_2O_7$-type oxides, whose crystal structure is also governed by ionic-radius ratio (r_A/r_B) of A-location and B-location. For $A_2B_2O_7$ oxides, the ionic radius ratio (r_A/r_B) between 1.46 and 1.78 helps to form stable pyrochlore-type structure, and the ionic-radius ratio below 1.46 can result in fluorite-type structure [20]. The r_A/r_B values of sintered samples can be obtained by Eq. (3), where $r(Ln^{3+})$ represents the ionic radius of Gd^{3+}, Yb^{3+} and Al^{3+}. The ionic radii of Gd^{3+}, Al^{3+}, Yb^{3+} and Ta^{5+} are 0.1053 nm, 0.0985 nm, 0.0535 nm and 0.068 nm, respectively.

$$r_A/r_B = \frac{2[r(\mathrm{Ln}^3)]}{r(Al^{3+}) + r(Ta^{5+})} \tag{3}$$

From Eq. (3), it can be obtained that the r_A/r_B values of Gd_2AlTaO_7 (1.73) and Yb_2AlTaO_7 (1.62) are in the range of 1.46–1.78. The computed result about ionic-radius ratio implies that the synthesized ceramics exhibit typical pyrochlore lattice, which agrees well with XRD spectrum displayed in Fig. 1.

Fig. 2 displays the representative micro-morphology of RE_2AlTaO_7 (RE = Gd and Yb) oxides. Clearly, the microstructure for the sintered samples is relatively dense, and the relative densities of Gd_2AlTaO_7 and

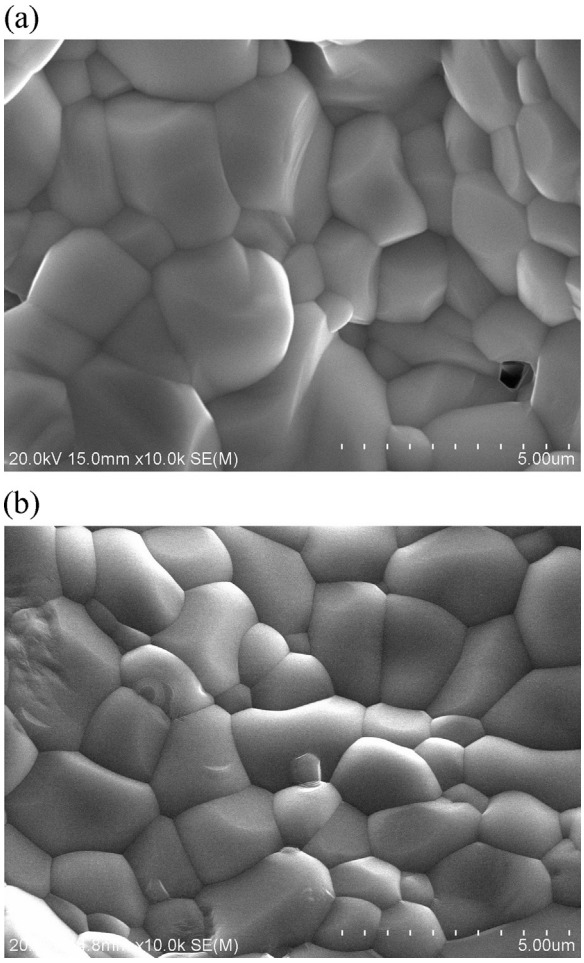

Fig. 2. Surface micro-morphology of sintered samples (a) Gd_2AlTaO_7 (b) Yb_2AlTaO_7.

Yb_2AlTaO_7 ceramics are 92.2% and 94.6%, respectively. The grain interfaces for Gd_2AlTaO_7 and Yb_2AlTaO_7 are spotless, no other materials or un-reacted raw reactants can be found. The crystal particle size of Gd_2AlTaO_7 is about 1–3 μm, and the crystal particle size of Yb_2AlTaO_7 is within 0.1–3.5 μm. From Fig. 3 and Table 1, it can be noted that the element compositions of the synthesized ceramics are consistent with the chemical formulas. The atomic ratio of $n_{Gd}:n_{Al}:n_{Ta}$ or $n_{Yb}:n_{Al}:n_{Ta}$ is close to 2:1:1, which is in agreement with chemical-formula of Gd_2AlTaO_7 or Yb_2AlTaO_7.

From Fig. 4, the calculated specific heat capacity of RE_2AlTaO_7 (RE = Gd and Yb) is in proportion to temperature, which can be fitted by Eqs. (4) and (5).

$$C_p(Gd_2AlTaO_7) = 0.38999 + 0.00006 \times T - 6280.84262/T^2 \tag{4}$$

$$C_p(Yb_2AlTaO_7) = 0.39277 + 0.00006 \times T - 6929.44142/T^2 \tag{5}$$

The thermal diffusivity of RE_2AlTaO_7 (RE = Gd and Yb) oxides tested via the laser-flash method is presented in Fig. 5. As can be noted from Fig. 5, the thermal diffusivity of RE_2AlTaO_7 (RE = Gd and Yb) ceramics is inversely proportional to temperature up to 1073 K, which exhibits typical phonon thermal-conducting behavior [21]. However, above 1073 K, the thermal diffusivity of Gd_2AlTaO_7 enhances slightly due to the influence of radioactive transport through the sample. The measured thermal diffusivities of Gd_2AlTaO_7 and Yb_2AlTaO_7 are within 0.45–0.91 mm^2/s, 0.32–0.38 mm^2/s, respectively.

The final computed thermal conductivity for RE_2AlTaO_7 (RE = Gd and Yb) oxides is presented in Fig. 6. Clearly, the thermal conductivity of RE_2AlTaO_7 (RE = Gd and Yb) oxides decreases with raising temperature before 1073 K. The elevated thermal conductivity above